Available online at www.sciencedirect.com

ScienceDirect

Journal of Computational and Applied Mathematics 215 (2008) 626–638

JOURNAL OF COMPUTATIONAL AND APPLIED MATHEMATICS

www.elsevier.com/locate/cam

Substructuring FE–XFE approaches applied to three-dimensional crack propagation

E. Wyart[a,*], M. Duflot[a], D. Coulon[b], P. Martiny[a], T. Pardoen[c], J.-F. Remacle[d], F. Lani[a]

[a] *Multiscale Materials Modeling Group, CENAERO, Avenue Mermoz 30, 6041 Gosselies, Belgium*
[b] *Numerical Methods and Optimisation Group, CENAERO, Avenue Mermoz 30, 6041 Gosselies, Belgium*
[c] *Department of Material Science and Processes, Université Catholique de Louvain, 1348 Louvain-la-Neuve, Belgium*
[d] *Department of Civil Engineering, Université Catholique de Louvain, Place du Levant 1, 1348 Louvain-la-Neuve, Belgium*

Received 23 August 2005

Abstract

Two substructuring methods are investigated in order to allow for the use of the eXtended Finite Element Method (X-FEM) within commercial finite element (FE) codes without need for modifying their kernel. The global FE problem is decomposed into two subdomains, the safe domain and the cracked domain based on the value of the level sets representing the crack. The safe domain is treated by the host FE software while the cracked domain is treated by an independent XFE code. The first substructuring method consists of calculating the Schur matrix of a cracked super-element with the XFE code. The second technique introduces the finite element tearing and interconnecting method (FETI) which ensures the compatibility of the displacements at the interface between the cracked and safe subdomains. The stiffness matrices and nodal forces are provided by the XFE and FE codes for the cracked and safe subdomains, respectively. The solutions obtained with these two techniques are rigorously equivalent to those computed with the stand-alone XFE code. First, the computational efficiency of the two approaches is demonstrated. Second, a validation is proposed towards comparison with reference values of the stress intensity factors in simple 3D cracked geometries. Finally, this contribution presents an application of the FE–XFE–FETI method to the computation of the stress intensity factor induced by a crack inside a hydraulic cylinder under internal pressure.

Keywords: X-FEM; FETI; Substructuring methods; Fracture mechanics

1. Introduction

The *eXtended Finite Element Method* (X-FEM) [11] is a numerical method which handles geometries containing singularities without the need of building a conforming mesh. It is based on the *partition of unity method* [10]. In addition, the *level set method* (LS) [17] is used as proposed in [18] to introduce the singularities into the geometry. The discontinuity in the displacement field is modelled with additional degrees of freedom (dofs) at nodes which have their support cut by the crack.

* Corresponding author.
E-mail address: eric.wyart@cenaero.be (E. Wyart).

0377-0427/$ - see front matter © 2007 Elsevier B.V. All rights reserved.
doi:10.1016/j.cam.2006.03.066

The X-FEM has been shown to provide good approximations of the stress intensity factors and crack paths, and is expected to be widely used in the near future by some of the majors of the aeronautics sector. To our knowledge the XFE and LS methods have not been implemented yet in general purpose finite element (FE) software. Indeed, such an implementation involves fundamental issues and programming difficulties. These difficulties depend on how deeply it is intended to modify the FE kernel. At this point, we can distinguish between two types of coding problems associated with:

- Specific theoretical features of the new methods compared with the classical FE method, for instance, the modification of the kinematics of the problem.
- The architecture of the host FE code which might not be flexible enough to allow for easy modifications. Among the limitations due to the particular architecture, we find, for instance, the difficulty to introduce "non-standard" dofs and the need for the dynamic allocation of dofs when considering the problem of crack propagation.

Indeed, generally, FE software can be seen as a set of four independent blocks:

- a block containing the materials constitutive laws (built-in or user-defined constitutive laws),
- a mesh manager (mesh generation, topology),
- a solvers manager,
- the core constituted of the kinematics (formulation).

In an ideally modular and perfectly interfaced FE code, each block can be modified or replaced by another block offering similar capabilities. First, most of the FE software are designed in such a way as to allow for the connection of a "materials" module (e.g., Z-MAT™ [22] or DIGIMAT™ [4] with ABAQUS™ [1]). Second, many commercial FE codes propose "mesh conversion" and /or "mesh import" tools, which make them relatively independent of the "mesh generation" module (e.g., ABAQUS™, NASTRAN™ [15], SAMCEF™ [16] are able to import meshes generated by common mesh-dedicated tools). On the contrary, even if most FE software propose several built-in solvers, it is very difficult for the user to connect his own external solver; this part is indeed generally closed. Finally, the kinematics are totally hidden and cannot be accessed by the user for modifications. Nevertheless, the possibility exists of introducing "user-defined elements" with proper kinematics. However, this feature is generally not flexible.

Following the objective of "minimal intervention" on the FE code, we decided to follow a multi-level or "code-coupling" approach. We aim at developing a set of libraries which facilitate the communication between an "unmodified" FE code and a stand-alone X-FEM-based code *before, during and after* the resolution of the problem. By definition, the "code-coupling" approach is strongly dependent on the *I/O* capabilities of both software.

In this work, we will critically assess two coupling methods belonging to the family of the so-called substructuring methods: the *super-element* method [3,12] and the *finite element tearing and interconnecting method* (FETI) [6]. In the framework of the "substructuring" methods, the cracked sample is decomposed into safe and cracked subdomains. The cracked and safe subdomains are treated by the XFE and FE codes, respectively.

Two other coupling methods could be envisaged but they are not exposed here. The first one is called the *homogenized crack tip method* (HCT) [20,21]. In this case, the cracked (i.e., discontinuous) medium is replaced by an homogeneous continuous medium of which the stiffness tensor is reduced. This is not a full implementation of the X-FEM. At the crack tip, a local problem is solved by the X-FEM at the scale of the material point and a reduced stiffness tensor is returned to the FE code through a "user material subroutine". For the second "code-coupling" method, a generic XFE element is implemented based on the "user element subroutine" provided by the host FE code. The elementary stiffness matrices are generated by the XFE code. This last method has not been implemented yet.

2. Theoretical background

2.1. Crack representation by the LS

The LS was introduced by Sethian [17] to model moving interfaces. A surface is represented by the zero level set of a function. Two "level sets" are needed for modelling a crack, the normal $\psi_n(\mathbf{x})$ and the tangent $\psi_t(\mathbf{x})$ "level sets".

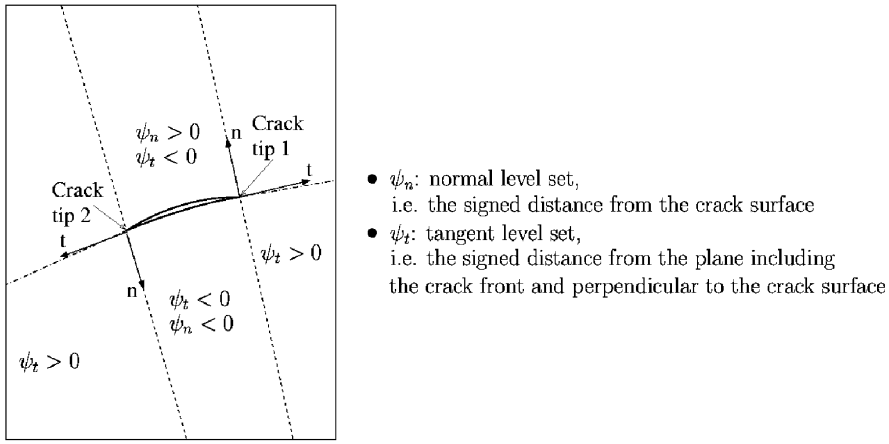

Fig. 1. Representation of a crack by two "level sets" ($\psi_{\mathrm{n}}(\mathbf{x})$ and $\psi_{\mathrm{t}}(\mathbf{x})$).

The function $\psi_{\mathrm{n}}(\mathbf{x})$ is the signed distance from the crack surface:

$$\psi_{\mathrm{n}}(\mathbf{x}) = \pm \min \|\mathbf{x} - \mathbf{x_n}\|, \tag{2.1}$$

where $\mathbf{x} \in \Omega$ and $\mathbf{x_n} \in \Gamma$ with Γ_{n} representing the crack surface; and $\psi_{\mathrm{t}}(\mathbf{x})$ is the signed distance from the plane including the crack front and perpendicular to the crack surface:

$$\psi_{\mathrm{t}}(\mathbf{x}) = \pm \min \|\mathbf{x} - \mathbf{x_t}\|, \tag{2.2}$$

where $\mathbf{x} \in \Omega$ and $\mathbf{x_t} \in \Gamma$ with Γ_{t} representing a plane including the crack front and perpendicular to the crack surface. The crack is defined as (see Fig. 1)

$$\{\mathbf{x} \in \Omega_{\mathrm{n}} | \psi_{\mathrm{n}}(\mathbf{x}) = 0, \psi_{\mathrm{t}}(\mathbf{x}) \leqslant 0\}. \tag{2.3}$$

The main advantage of this approach is that singularities and/or discontinuities can be added without modifying the mesh or the Computer Assisted Design (CAD).

2.2. The eXtended finite element method

The X-FEM is based on the *partition of unity method* [10]. In this frame, an *a priori* knowledge of the solution can be introduced in the FE approximation through an enrichment of the shape functions space. Two types of enrichment are considered for fracture mechanics problems:

- In order to model the discontinuity of the displacement field, it is natural to enrich the approximation space with the products of the nodal shape functions by the Heaviside function, which is defined as

$$H(\mathbf{x}) = \begin{cases} -1 & \text{if } \psi_{\mathrm{n}} \leqslant 0^-, \\ 1 & \text{if } \psi_{\mathrm{n}} \geqslant 0^+. \end{cases} \tag{2.4}$$

- In order to improve the accuracy of the solution at the crack tip and in certain cases increase the convergence rate [2,8], the theoretical asymptotic solution for the displacement around the crack tip is added in the formulation. The approximation space is enriched with the product of the crack tip enrichment functions F^l (where $l = 1, \ldots, 4$) provided by the singular term of the linear elastic fracture mechanics (LEFM) [19] displacement field expansion

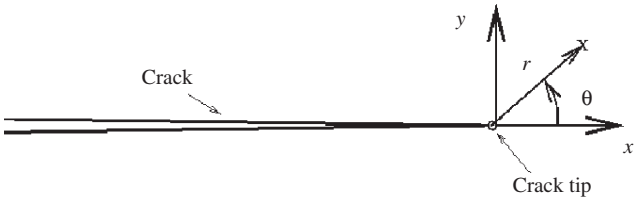

Fig. 2. Polar coordinates system attached to the crack tip.

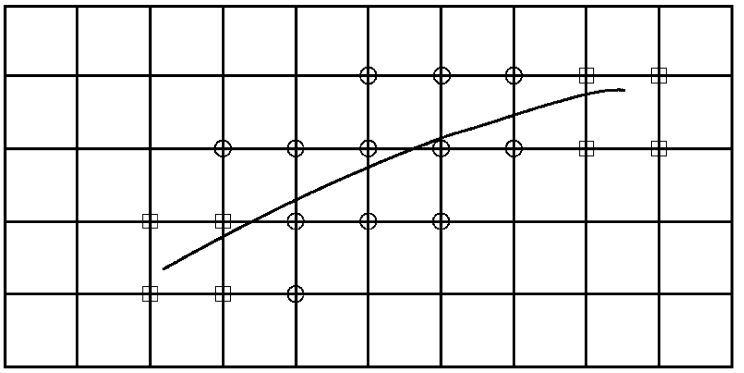

Fig. 3. Inserting a crack on a regular, non-conforming mesh. The squares represent nodes which have dofs enriched with the crack tip solution of LEFM. The nodes surrounded by a circle must have dofs enriched with the Heaviside function.

and the nodal shape functions:

$$\{F^l\} \equiv \left\{ \sqrt{r}\sin\left(\frac{\theta}{2}\right), \sqrt{r}\cos\left(\frac{\theta}{2}\right), \sqrt{r}\sin\left(\frac{\theta}{2}\right)\cos(\theta), \sqrt{r}\cos\left(\frac{\theta}{2}\right)\sin(\theta) \right\}, \tag{2.5}$$

where (r, θ) is the local polar coordinates system for a reference frame attached to the crack tip (Fig. 2).

Finally, the displacement field becomes in the extended FE formulation:

$$u^h(\mathbf{x}) = \underbrace{\boxed{\sum_{i\in I} u_i \phi_i(\mathbf{x})}}_{\text{Classical FE approximation}} + \underbrace{\boxed{\sum_{j\in J} b_j \phi_j(\mathbf{x}) H(\mathbf{x})}}_{\text{Crack opening}} + \underbrace{\boxed{\sum_{k\in K_1, K_2} \phi_k(\mathbf{x}) \sum_{l=1}^{4} c_k^l F^l(\mathbf{x})}}_{\text{Crack tip solution}}, \tag{2.6}$$

where

- I is the set of all nodes of the domain.
- J is the set of nodes whose support is cut by a crack (circle nodes in Fig. 3).
- K_1 and K_2 are the set of nodes containing the first and the second crack tip, respectively (square nodes in Fig. 3).
- u_i are the usual dofs (i.e., displacement) for node i.
- ϕ_i is the shape function associated to node i.
- b_j are the additional dofs associated with the Heaviside function. These dofs give the jump in the displacement field across the crack at node j. If the crack and the mesh coincide, b_j represent the crack opening.
- $c_{k_1}^l$ and $c_{k_2}^l$ are the additional dofs associated with the crack tip enrichment functions. Unlike b_j, these dofs have no evident physical meaning.

Only a set of nodes can be enriched. If every node of the mesh is enriched, linear dependency between equations occurs and the global stiffness matrix becomes singular. It must be noted that the elementary stiffnesses of enriched elements must be integrated with special Gauss rules [11].

3. Substructuring FE–XFE approach

3.1. Decomposition of the domain

As a prerequisite to the use of the substructuring methods, we need to proceed to the decomposition of the domain. A crack is introduced in an FE mesh by means of "level sets". The mesh is decomposed into two subdomains:

- the safe or defect free subdomain, "treated" by the FE software,
- the cracked domain, "treated" by the XFE code.

The procedure is illustrated in Fig. 4. Two kinds of decomposition are defined:

- A "level set"-based domain decomposition. This decomposition is based on the value of the normal and tangent "level sets" and the characteristic length of the mesh. This decomposition is used with the FETI method (see Section 3.3) and also for the *post processing* of the super-element (see Section 3.2).[1]

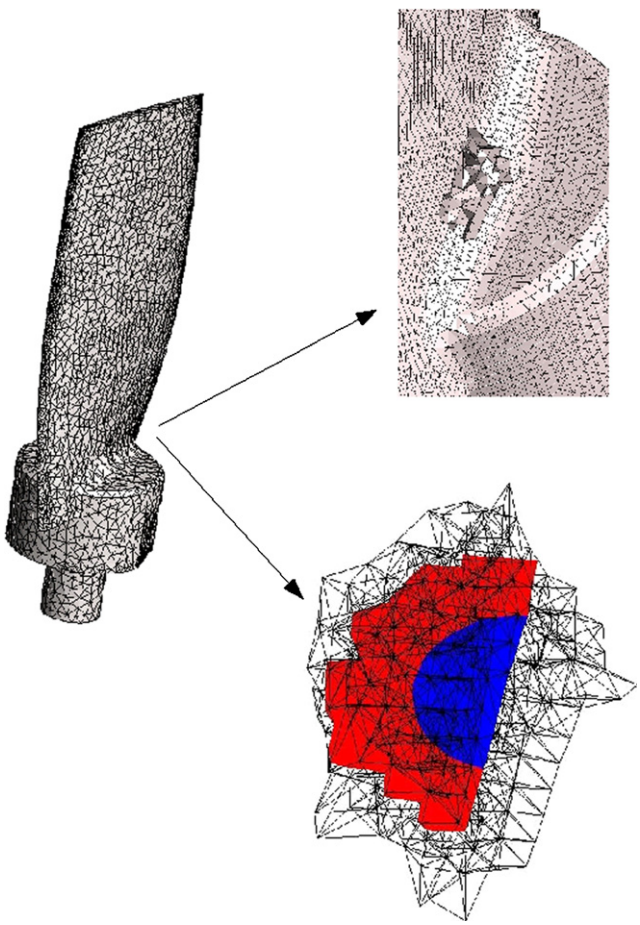

Fig. 4. Decomposition of an arbitrary mesh into a safe domain and a cracked domain based on the normal and the tangent "level sets" of a semi-circular crack.

[1] Indeed, the subdomain must include the contour of the equivalent domain integral [13,14] for the computation of the stress intensity factor.

- A minimum domain decomposition. The boundary of each cracked domain is the first layer of non-enriched nodes found when moving away from the crack. With this decomposition, the number of boundary and internal dofs are minimized, reducing the computation time of the Schur complement and minimizing the bandwidth of the global matrix (see Section 3.2).

3.2. Super-element

The coupling of an FE software and an XFE code by using super-elements was first proposed by Bordas [3]. The method consists in decomposing the problem into a safe domain and one or several cracked domains and in treating either the safe or the cracked domain as a super-element. In this case, the XFE code is used to build the Schur complement of the cracked domain. The global problem can be written as

$$\mathbf{K_G u_G} = \begin{pmatrix} \mathbf{K_{sd}} & \mathbf{K_{sc}} \\ \mathbf{K_{cs}} & \mathbf{K_{cd}} \end{pmatrix} \begin{pmatrix} \mathbf{u_{sd}} \\ \mathbf{u_{cd}} \end{pmatrix} = \begin{pmatrix} \mathbf{f_{sd}} \\ 0 \end{pmatrix}, \tag{3.1}$$

where $\mathbf{K_G}$ is the stiffness matrix of the complete problem, $\mathbf{K_{sd}}$ is the stiffness matrix associated to the dofs of the safe domain only (including its interface with the cracked domain), $\mathbf{K_{cd}}$ is the stiffness matrix of the cracked domain (including the interface with the safe domain), $\mathbf{K_{sc}} = \mathbf{K_{cs}^T}$ is the stiffness matrix coupling the dofs of the safe domain and the nodes of the interface and $\mathbf{f_{sd}}$ is the vector of forces applied to the nodes of the safe domain.

Note that we assumed that no forces are applied neither on the boundary nor in the interior of the cracked domain. This assumption is required by the super-element format used.[2] The vector $\mathbf{u_{sd}}$ contains the dofs of the *safe domain*. The dofs of the *cracked domain* $\mathbf{u_{cd}}$ are split into the interior dofs $\mathbf{u_I}$ and the boundary dofs $\mathbf{u_B}$:

$$\mathbf{K_{cd} u_{cd}} = \begin{pmatrix} \mathbf{K_{BB}} & \mathbf{K_{BI}} \\ \mathbf{K_{IB}} & \mathbf{K_{II}} \end{pmatrix} \begin{pmatrix} \mathbf{u_B} \\ \mathbf{u_I} \end{pmatrix} = \begin{pmatrix} \mathbf{0} \\ \mathbf{0} \end{pmatrix}, \tag{3.2}$$

where $\mathbf{K_{II}}$ is the stiffness matrix linking the interior dofs, $\mathbf{K_{BB}}$ is the stiffness matrix linking the boundary dofs and $\mathbf{K_{IB}} = \mathbf{K_{BI}^T}$ is the stiffness matrix linking internal and boundary dofs. Note again that $\mathbf{u_B}$ cannot include enriched dofs while $\mathbf{u_I}$ can. The $\mathbf{u_I}$ dofs are thus eliminated by condensation and the matrix $\mathbf{K_{cd}}$ is replaced by its Schur complement $\mathbf{K_{Schur}}$ in the global stiffness matrix $\mathbf{K_G}$:

$$\mathbf{K_{Schur}} = \mathbf{K_{BB}} - \mathbf{K_{BI}} \mathbf{K_{II}^{-1}} \mathbf{K_{IB}}. \tag{3.3}$$

Because the internal dofs of the cracked domain are not coupled with the dofs of the safe domain, $\mathbf{K_{sc}}$ can be rewritten as

$$\mathbf{K_{sc}} = (\mathbf{K_{sB}} \quad \mathbf{0}), \tag{3.4}$$

where $\mathbf{K_{sB}}$ is the coupling matrix between the dofs of the safe domain and the boundary dofs.

The global problem can be recast in the form

$$\mathbf{K_G u_G} = \begin{pmatrix} \mathbf{K_{sd}} & \mathbf{K_{sB}} \\ \mathbf{K_{Bs}} & \mathbf{K_{Schur}} \end{pmatrix} \begin{pmatrix} \mathbf{u_{sd}} \\ \mathbf{u_B} \end{pmatrix} = \begin{pmatrix} \mathbf{f_{sd}} \\ \mathbf{0} \end{pmatrix} \tag{3.5}$$

which is solved by the host FE code.

The Schur complement of a substructure is generally dense. Assembling $\mathbf{K_{Schur}}$ in the global stiffness matrix implies a change in the sparsity of the latter. First, it is of the uttermost importance to reduce the memory needed for and the computational cost associated with the computation of the Schur complement. Second, it is recommended to limit the size of the Schur complement as it has a dramatic effect on the sparsity of the global system. That is why we choose a minimal domain decomposition for the cracked domain with the boundary composed by the first layer of non-enriched nodes.

To compute the value of the stress intensity factors at the crack tip, the displacement field must be known in the vicinity of the crack tip. A new domain is defined with a size such that it contains the contour of the interaction integral.

[2] Indeed, the PERMAS format available in SAMCEF™ was chosen for the first simple applications.

Then an XFE problem is solved on this domain with the result computed in Eq. (3.5) as Dirichlet boundary conditions. Finally, the stress intensity factors are computed using the interaction integral with the help of the level sets of the crack.

3.3. Coupled FEM/X-FEM based on the FETI method

3.3.1. Introduction

The FETI is a substructuring method. The FETI method has been developed to handle and solve large-scale problems. FETI allows both parallel and sequential computation schemes. According to [9], computational time and memory requirements are, respectively, one to two orders of magnitude lower than those of a direct solver.

The whole domain is divided into several substructures, the problem to be solved is reduced to an interface problem. The stiffness matrices and the nodal forces are extracted from the subdomains. The global system is solved by means of the FETI method.

3.3.2. Mathematical formulation

The following section is inspired by the work of Farhat et al. [6].

Let us consider a domain Ω. The system to be solved is

$$\mathbf{K}\mathbf{u} = \mathbf{f}, \tag{3.6}$$

where $\mathbf{K}$ is the stiffness matrix (symmetric semi-definite positive) on the domain Ω, $\mathbf{u}$ is the nodal displacement vector and $\mathbf{f}$ is the vector of prescribed forces.

The domain Ω is divided into N_s disconnected subdomains Ω_s. FETI consists in replacing Eq. (3.6) by

$$\begin{aligned} &\mathbf{K}^{(s)}\mathbf{u}^{(s)} = \mathbf{f}^{(s)} - \mathbf{B}^{(s)\mathrm{T}}\boldsymbol{\lambda} \quad \text{with } s = 1, \ldots, N_s, \\ &\Delta = \sum_{s=1}^{N_s} \mathbf{B}^{(s)}\mathbf{u}^{(s)} = \mathbf{0}, \end{aligned} \tag{3.7}$$

where $\mathbf{K}^{(s)}$ and $\mathbf{f}^{(s)}$ are the contributions from the subdomain $\Omega^{(s)}$, respectively, to $\mathbf{K}$ and $\mathbf{f}$, $\boldsymbol{\lambda}$ is a vector of Lagrange multipliers and $\mathbf{B}^{(s)}$ is a signed boolean matrix for the localization of the dofs on the interface. The Lagrange multipliers are introduced to enforce continuity of the displacements on the boundary $\Gamma^{(s)}$ of the subdomain (i.e., $\Delta = \mathbf{0}$ on $\Gamma^{(s)}$).

Generally, a mesh partition can contain $N_\mathrm{f} \leqslant N_s$ floating substructures (i.e., substructures with an insufficient number of essential boundary conditions to avoid the singularity of the matrix $\mathbf{K}^{(s)}$). Therefore, the N_f equilibrium problems

$$\mathbf{K}^{(s)}\mathbf{u}^{(s)} = \mathbf{f}^{(s)} - \mathbf{B}^{(s)\mathrm{T}}\boldsymbol{\lambda}, \quad s = 1, \ldots, N_\mathrm{f}. \tag{3.8}$$

are ill-posed. To make the problem properly conditioned, it must be verified that

$$(\mathbf{f}^{(s)} - \mathbf{B}^{(s)\mathrm{T}}\boldsymbol{\lambda}) \perp \mathrm{Ker}(\mathbf{K}^{(s)}), \quad s = 1, \ldots, N_\mathrm{f}, \tag{3.9}$$

and the solution of Eq. (3.8) must be computed as

$$\mathbf{u}^{(s)} = \mathbf{K}^{(s)+}(\mathbf{f}^{(s)} - \mathbf{B}^{(s)\mathrm{T}}\boldsymbol{\lambda}) + \mathbf{R}^{(s)}\boldsymbol{\alpha}^{(s)}, \tag{3.10}$$

where $\mathbf{K}^{(s)+}$ is a generalized inverse of $\mathbf{K}^{(s)}$, $\mathbf{R}^{(s)} = \mathrm{Ker}(\mathbf{K}^{(s)})$ is the kernel of $\mathbf{K}^{(s)}$ (rigid body modes) and $\boldsymbol{\alpha}$ is a vector containing a maximum of six constants. The introduction of the unknowns $\boldsymbol{\alpha}^{(s)}$ is compensated by the new equations resulting from Eq. (3.9):

$$\mathbf{R}^{(s)\mathrm{T}}(\mathbf{f}^{(s)} - \mathbf{B}^{(s)\mathrm{T}}\boldsymbol{\lambda}) = \mathbf{0}, \quad s = 1, \ldots, N_\mathrm{f}. \tag{3.11}$$

Substituting Eq. (3.10) in Eq. (3.7) and using Eq. (3.11), the FETI interface problem leads to

$$\begin{bmatrix} \mathbf{F_I} & -\mathbf{G_I} \\ -\mathbf{G_I}^\mathrm{T} & \mathbf{0} \end{bmatrix} \begin{bmatrix} \boldsymbol{\lambda} \\ \boldsymbol{\alpha} \end{bmatrix} = \begin{bmatrix} \mathbf{d} \\ -\mathbf{e} \end{bmatrix}, \tag{3.12}$$

where

$$\begin{aligned}
&\mathbf{F_I} = \sum_{s=1}^{N_s} \mathbf{B}^{(s)}\mathbf{K}^{(s)+}\mathbf{B}^{(s)\mathrm{T}},\\
&\mathbf{G_I} = [\mathbf{B}^{(1)}\mathbf{R}^{(1)} \quad \cdots \quad \mathbf{B}^{(N_\mathrm{f})}\mathbf{R}^{(N_\mathrm{f})}],\\
&\boldsymbol{\alpha}^{\mathrm{T}} = [\boldsymbol{\alpha}^{(1)\mathrm{T}} \quad \cdots \quad \boldsymbol{\alpha}^{(N_\mathrm{f})\mathrm{T}}]^{\mathrm{T}},\\
&\mathbf{d} = \sum_{s=1}^{N_s} \mathbf{B}^{(s)}\mathbf{K}^{(s)+}\mathbf{f}^{(s)},\\
&\mathbf{e}^{\mathrm{T}} = [\mathbf{R}^{(1)}\mathbf{f}^{(1)\mathrm{T}} \quad \cdots \quad \mathbf{R}^{(N_\mathrm{f})}\mathbf{f}^{(N_\mathrm{f})\mathrm{T}}]^{\mathrm{T}}.
\end{aligned} \tag{3.13}$$

If Ω_s is not a floating substructure, then $\mathbf{K}^{(s)+} = \mathbf{K}^{(s)-1}$. The operator $\mathbf{F_I}$ is the sum of independent substructure matrices and its size is equal to the number of Lagrange multipliers. Under certain conditions (see [7]), the matrix $\mathbf{F_I}$ can be interpreted as the sum of the inverse of the subdomain Schur complements:

$$\mathbf{F_I} = \sum_{s=1}^{N_s} \mathbf{S}_{\mathbf{bb}}^{(s)^{-1}}, \tag{3.14}$$

$$\mathbf{S}_{\mathbf{bb}}^{(s)} = \mathbf{K}_{\mathbf{bb}}^{(s)} - \mathbf{K}_{\mathbf{bi}}^{(s)}\mathbf{K}_{\mathbf{ii}}^{-1^{(s)}}\mathbf{K}_{\mathbf{ib}}^{(s)}. \tag{3.15}$$

Generally, $\mathbf{F_I}$ is symmetric semi-definite positive, allowing the use of a preconditioned conjugate gradient solver method (PCG) to solve Eq. (3.12).

4. Numerical experiments and validation

4.1. Description of the sample

A 3D bar with an inclined crack is studied for various misorientation angles. The stress intensity factors are computed along the crack front and compared with those obtained with a meshless code.[3]

The sample is shown in Fig. 5. The upper face is submitted to a tensile stress and the bottom face is fixed in the z-direction. To avoid singularity of the global matrix, one edge parallel with the x-axis and one edge parallel with the y-axis are fixed in the y-direction and z-direction, respectively.

- $a/W = 0.2$,
- $H/W = 2$,
- $T = 100$,
- $\sigma = 1.0\,\mathrm{Pa}$,
- θ varies from $0°$ to $90°$.

4.2. Numerical results

We treat the FETI and the super-element coupling methods together, using the same mesh. The computed solutions are rigorously identical to the reference XFE solution. Indeed, the same global matrix is solved and only the solver accuracy can influence the quality of the solution.

The arithmetic mean values of the stress intensity factors along the crack fronts are compared with those coming from the meshless code. The values of the stress intensity factors near the external boundaries of the sample are not taken into account because the domain of the integral is not large enough (the zones A and A′ in Fig. 7).

Fig. 6 shows that the mode I stress intensity factors are in a very good agreement with the mode I computed by the meshless code. Nevertheless, the mean values of K_{II} (left side of Fig. 6) are overestimated for low values of θ. This is due to the fact that K_{II} along the crack front is not homogeneous (see Fig. 7). The principal reason is the existence of

[3] There are no analytical solutions available for this crack configuration described in [5].

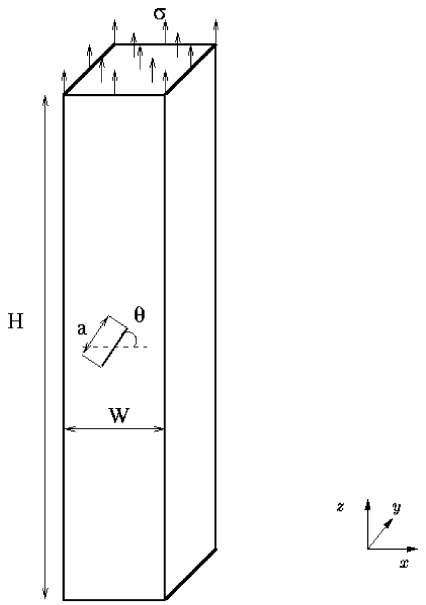

Fig. 5. Inclined crack in 3D bar.

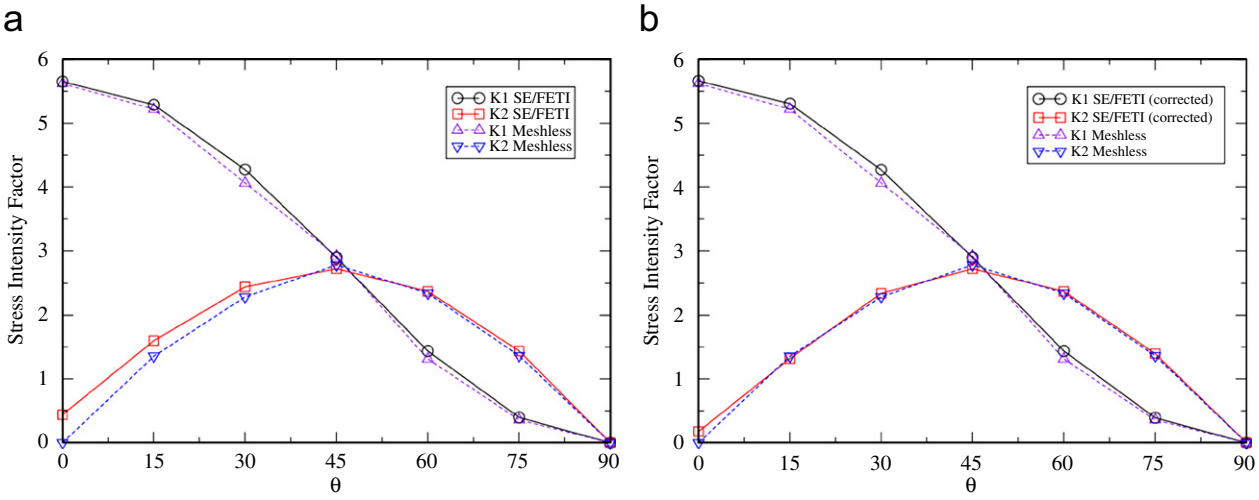

Fig. 6. Uncorrected (a) and corrected (b) stress intensity factors in modes I and II with substructuring methods.

spurious stress concentrations in the vicinity of the crack tip. These stress concentrations occur when an element is cut in such a way that there is a very small volume of the element on one side of the crack. These stress concentrations can be interpreted as "mesh locking". Moreover, K_{II} is oscillating around a mean value. This oscillation along the crack front have been also observed for the mode I. They are related to the Gauss quadrature rules which are not suited for integrating $1/r$ fields.

If these erroneous values of K_{II} are eliminated (by hand), the agreement with the reference values is good (see the right side of Fig. 6). The maximum relative difference between the values obtained with the substructuring method and the reference values is less than 5%. As the number of elements involving a spurious stress is relatively low, refining the mesh in the vicinity of the crack tip allows for an accurate computation of the global stress intensity factors. Indeed the

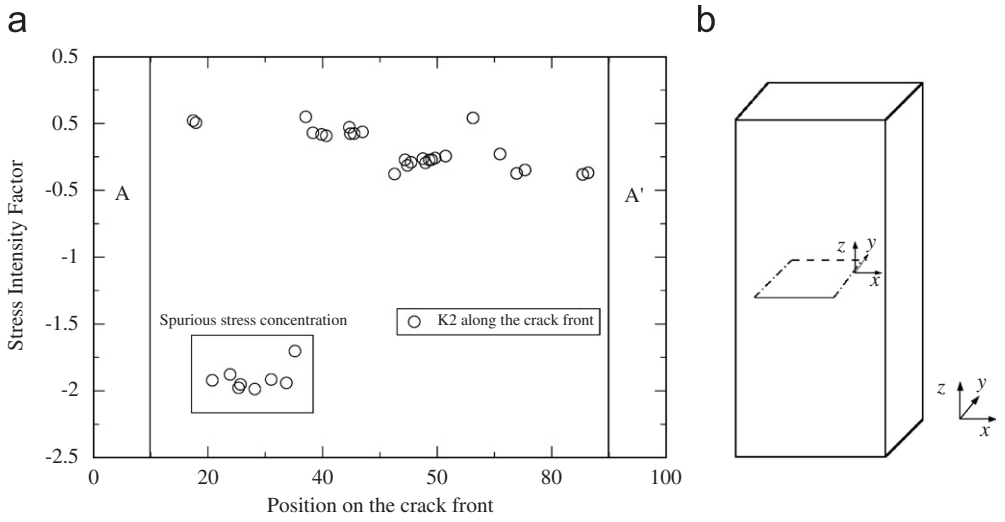

Fig. 7. K_{II} along the crack front for $\theta = 0$ (a) and the representation of the crack (b).

volume of the concerned elements becomes small compared to the domain of the equivalent domain integral. However, this solution did not fix the problem of spurious stress and, locally, the stress intensity factor can still be erroneous.

4.3. Comments on the methods

For large problems, the computation of the Schur complement can be too expensive in terms of computational time and memory requirement. Indeed, these are related to the size and boundary of the super-element domain. Moreover, the bandwidth of the global system solved in the FE software is larger. It is equal to the number of dofs on the boundary of the subdomain. As a consequence, the solver is slowed down.

Compared to the FETI method for a problem that involves about 120,000 dofs, the computational time for the super-element method is three to four times bigger and the maximum allocatable memory is used. The use of the super-element method is more judicious for small crack problems.

In order to accelerate the computation of the Schur complement, only the lower triangle matrix is computed and the sparsity of the $\mathbf{K_{bi}}$ matrix is used to reduce the number of operations in the product $\mathbf{K_{bi}}\mathbf{K_{ii}}^{-1}\mathbf{K_{ib}}$.

5. Application

5.1. Description of the model

We apply the method to the computation of the stress intensity factors along the front of a crack located inside a hydraulic cylinder under internal pressure. This study was realized in the framework of the European Commission Integrated Project PROHIPP (new design and manufacturing processes for high-pressure fluid power products). Fig. 8 shows the Von Mises stress inside the cylinder. The hoop stress near the oil port is detailed in Fig. 9. Indeed, the stress is maximum in the plane of symmetry where a crack has been experimentally observed.

As a first approximation, we focus on the part of the cylinder around the oil port where we compute the stress intensity factors. This zoom is required since the mesh of the whole cylinder is far too coarse for a small crack analysis. Fig. 10 shows the model used for the computation. The cylinder is made of steel (Young modulus = 210 GPa and Poisson ratio = 0.3). The inner pressure is equal to 10 MPa. The hole inserted at the center of the cylinder has a radius of 5 mm. An axial stress σ_z is added according to the relation:

$$\sigma_z = \frac{Pr}{2t} \tag{5.1}$$

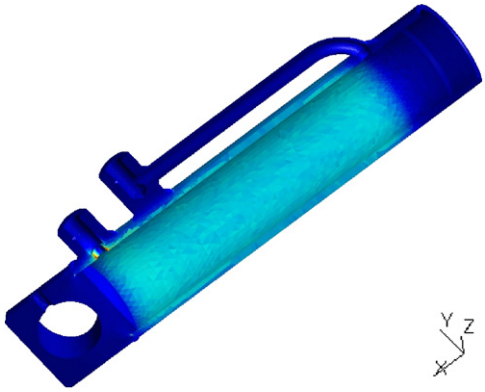

Fig. 8. Von Mises stress inside the hydraulic cylinder under internal pressure.

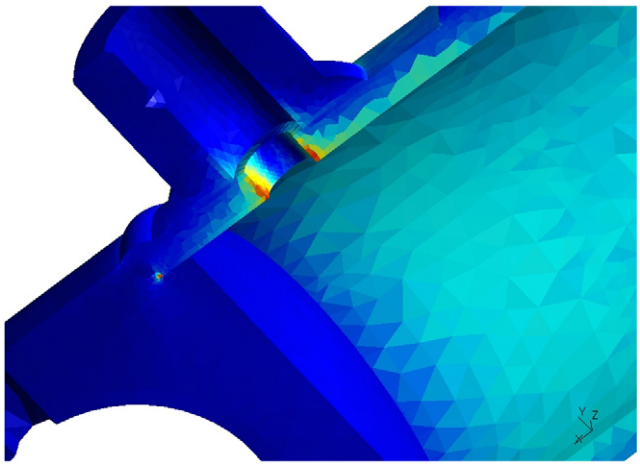

Fig. 9. Zoom on the oil port of the hydraulic cylinder. Stress concentration can be observed at the bottom of the oil port.

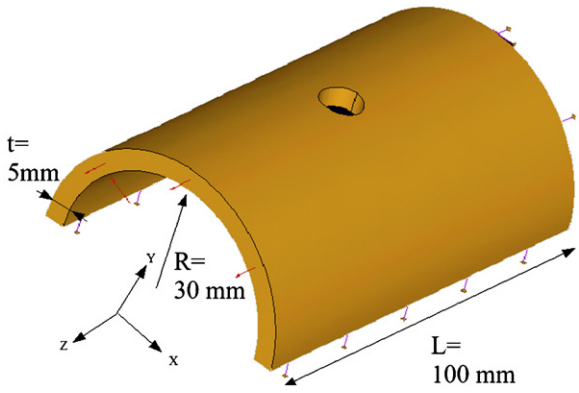

Fig. 10. Model used for the computation.

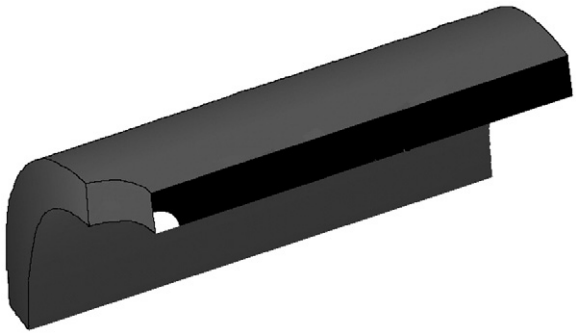

Fig. 11. Representation of the crack (in white) inserted in the symmetry plane of the cylinder.

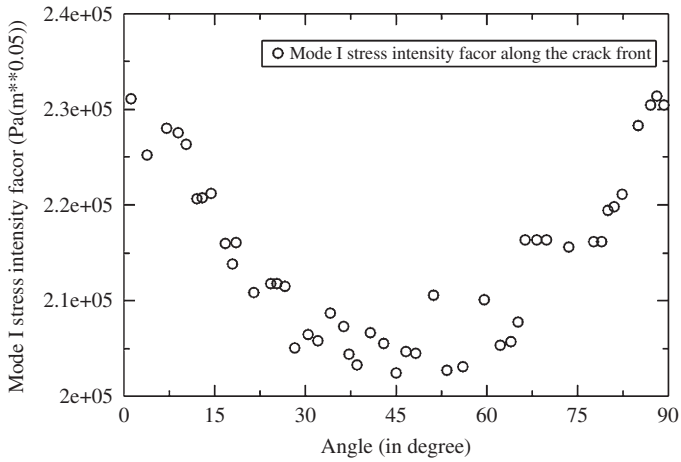

Fig. 12. Mode I stress intensity factor along the crack front.

on the front face ($z = 100$) of the model. To avoid rigid body motions, the rear face ($z = 0$) is fixed along the z-direction, the bottom faces are fixed along the y-direction. One of the nodes located at the intersection between the symmetry plane and the rear face is fixed along the x-direction.

A circular crack is inserted in the symmetry plane (see Fig. 11). The radius of the crack is 2.5 mm and its center is located at $x = 0$, $y = 27.5$, $z = -45$ mm.

5.2. Results

Fig. 12 shows the stress intensity factor computed along the crack front. As the crack is in a symmetry plane, only the mode I is present. These results correspond to the typical variation of the stress intensity factor along the front, with the highest values at the free surfaces where the state is close to plane stress conditions.

6. Conclusions and prospects

The X-FEM and the LS methods are promising methods in modelling fracture mechanics problems. Nevertheless, these methods are not yet available in commercial software due to some inherent theoretical and implementational difficulties of the methods.

In this context, two substructuring FE–XFE-based methods were developed: the super-element method and the FETI method. These methods give very promising results except for the overestimation of the stress intensity factor K_{II}

related to spurious stress concentration for the problem of inclined crack. Those peaks are related to basic issues related to the X-FEM.

Compared to the super-element method, FETI is much cheaper in terms of required memory and also faster in the case of problems with more than 100,000 dofs. However, if for a given crack configuration, multiple load cases must be treated, the super-element must be computed only once which makes it competitive with FETI.

In the near future, the FETI method will be applied to crack analysis on the outer skin of a structural part modelled with shells. In this case, a local plane stress formulation is defined on the cracked subdomain under the assumption that out-of-plane loading can be neglected.

Acknowledgments

The authors are grateful to Nicolas Moës for providing his X-FEM code. This research was funded by the Walloon Region and FEDER European funds under contract no. EP1A122030000102.

References

[1] ABAQUS, A General-Purpose Finite Element Program, Hibbitt, Karlsson and Sorensen, Pawtucket, RI, USA, 2005.
[2] E. Béchet, H. Minnebo, N. Moës, B. Burgardt, Improved implementation and robustness study of the X-FEM method for stress analysis around cracks, Internat. J. Numer. Methods Eng. 64 (2005).
[3] S. Bordas, eXtended Finite Element Method for elastic and elastic–plastic cracks in complex component, Proposal for the FAA contract DTFA03-98-F-IA025, 2001.
[4] DIGIMAT, Software for the linear and non-linear multiscale modeling of heterogeneous materials. ⟨http://www.e-xstream.com/en/digimat.asp⟩.
[5] M. Duflot, Application des méthodes sans maillage à la mécanique de la rupture, Ph.D. Thesis, Université de Liège, Liège, 2004.
[6] C. Farhat, J. Mandel, The two-level FETI method for static and dynamic plate problems. Part I: an optimal iterative solver for biharmonic systems, Comput. Methods Appl. Mech. Eng. 155 (1998) 129–151.
[7] C. Farhat, F.X. Roux, Implicit parallel processing in structural mechanics, Comput. Mech. Adv. 2 (1994) 1–124.
[8] P. Laborde, J. Pommier, Y. Renard, M. Salaün, High order extended finite element method for cracked domain, Internat. J. Numer. Methods Eng. 64 (2005).
[9] M. Lesoinne, K. Pierson, An efficient FETI implementation on distributed shared memory machine with independent numbers of subdomains and processors, Contemp. Math. 218 (1998).
[10] J.M. Melenk, I. Babuška, The partition of unity finite element method: basic theory and application, Comput. Methods Appl. Mech. Eng. 39 (1996) 289–314.
[11] N. Moës, J. Dolbow, T. Belytschko, A finite element method for crack growth without remeshing, Internat. J. Numer. Methods Eng. 46 (1999) 131–150.
[12] B. Moran, S. Bordas, J.G. Conley, Damage tolerance assessment of complex aerospace structures, Federal Aviation Administration Report, Design and quality assurance of premium quality aerospace castings, FAA contract, 2004.
[13] B. Moran, C.F. Shih, A general treatment of crack tip contour integrals, Internat. J. Fracture 35 (1987) 295–310.
[14] B. Moran, C.F. Shih, Crack tip and associated domain integrals from momentum and energy balance, Eng. Fracture Mech. 27 (1987) 615–642.
[15] MSC.NASTRAN, General purpose finite element software. ⟨http://www.mscsoftware.com/⟩.
[16] SAMCEF, General purpose finite element analysis package. ⟨http://www.samcef.com⟩.
[17] J.A. Sethian, in: Level Set Methods and Fast Marching Methods: Evolving Interfaces in Computational Geometry Fluid Mechanics Computer Vision and Material Science, Cambridge University Press, Cambridge, UK, 1999.
[18] M. Stolarska, D.L. Chopp, N. Moës, T. Belytschko, Modeling crack growth by level sets and the extended finite element method, Internat. J. Numer. Methods Eng. 51 (2001) 943–960.
[19] S. Suresh, Fatigue of Materials, second ed., Cambridge University Press, Cambridge, UK, 1998.
[20] E. Wyart, P. Martiny, J.-F. Remacle, T. Pardoen, F. Lani, Hierarchical approaches for the calculation of stress intensity factor, in: Junior Euromat, Lausanne, 2004.
[21] E. Wyart, P. Martiny, J.-F. Remacle, T. Pardoen, F. Lani, Multi-scale approaches for the simulation of cracks, in: The 11th International Congress of Fracture, Turin, 2005.
[22] Z-MAT, A user-extendable, object-oriented material modeling library and development environment for use in mechanical behavior simulation, characterization, and finite element analysis. ⟨http://www.nwnumerics.com/Z-mat/⟩.